ELSEVIER

Biochimica et Biophysica Acta 1509 (2000) 245–254

BIOCHIMICA ET BIOPHYSICA ACTA
BBA

www.elsevier.com/locate/bba

Effect of low external calcium on the ERG current of NG108-15 cells

Hans Meves *

I. Physiologisches Institut der Universität des Saarlandes, D-66421 Homburg-Saar, Germany

Received 17 March 2000; received in revised form 27 July 2000; accepted 28 July 2000

Abstract

K^+ currents through ERG (*ether-à-go-go* related gene) channels were recorded in whole-cell voltage clamped NG108-15 neuroblastoma × glioma hybrid cells. The channels were fully activated by low holding potential ($V_H = -20$ mV) and long depolarizing prepulses. Hyperpolarizing pulses elicited inward currents which deactivated after reaching a peak. Lowering $[Ca^{2+}]_o$ from 5 to 1.5 or 0.5 mM decreased τ^{-1}, the rate constant of deactivation. The effect can be explained by a shift of the $\tau^{-1}(V)$ curve to more negative potentials caused by an increase in surface charge density. Plotting τ^{-1} against $[Ca^{2+}]_o$ for different potentials yielded straight lines; their slope was independent of potential at −140 to −120 mV and decreased at more positive potentials. The time to peak curve and the maximum of the steady-state inward current were also shifted to more negative potentials. In addition, peak ERG inward current increased. Raising $[Ca^{2+}]_o$ from 5 to 10 mM accelerated deactivation and decreased the peak current. 5 mM Ba^{2+} affected τ^{-1} similarly and inhibited peak current more strongly whereas 5 mM Mg^{2+} was less potent. As found by Faravelli et al. (J. Physiol. 496 (1996) 13), bath solutions devoid of divalent cations (0 Ca^{2+}, 0 Mg^{2+}, 0.1 or 1.1 mM EGTA) abolished deactivation almost completely. The phenomenon was seen with bath containing either 40 or 6.5 mM K^+. Its occurrence was favored by raising the temperature to 34°C. It suggests a particular requirement of channel closing for Ca^{2+}.

Keywords: ERG current; NG108-15 cell; Deactivation; Calcium; Surface charge

1. Introduction

In ERG (*ether-à-go-go* related gene) potassium channels, activation and deactivation are much slower than inactivation and recovery from inactivation, giving rise to the characteristic rectification-like behavior of these channels [1–3]. The ERG current of rat dorsal root ganglion × mouse neuroblastoma hybrid cells (clone F11) fails to deactivate in bath solution with 120 mM K^+ devoid of divalent cations [4]. Likewise, the delayed rectifier current in rabbit sino-atrial node cells which is encoded by ERG hardly deactivates in Ca^{2+}- and Mg^{2+}-free bath with 140 mM K^+ [5]. Contrary to these observations, ERG channels expressed in Chinese hamster ovary cells retain deactivation gating in bath with 4 mM K^+ free of divalent cations [6].

Three hypotheses are discussed to explain the extreme slowing of deactivation in Ca^{2+}- and Mg^{2+}-free bath: (a) increase in surface charge density, (b) absence of a cofactor for channel closing, and (c) absence of blocking ions. Divalent cations screen negative surface charges, thereby altering the potential across the membrane [7]. In the absence of Ca^{2+} and Mg^{2+} the curve relating time or rate constant of

* Fax: +49-6841-166468;
E-mail: phhmev@med-rz.uni-sb.de

0005-2736/00/$ – see front matter
PII: S0005-2736(00)00302-3

deactivation to potential (e.g., Fig. 9C of [8]) would be strongly shifted in the hyperpolarizing direction. The cofactor hypothesis [9] assumes that Ca^{2+} is a necessary cofactor for the closing of K^+ channels. In the view of Ho et al. [5], deactivation is not an intrinsic property of the ERG channel but results from voltage-dependent blockage by Ca^{2+} and Mg^{2+}. Consequently, it is absent in Ca^{2+}- and Mg^{2+}-free bath.

I recorded the ERG current of NG108-15 neuroblastoma×glioma hybrid cells in Mg^{2+}-free bath solutions with different Ca^{2+} concentrations and tried to distinguish between these three hypotheses. I find that most effects of a Ca^{2+}-poor bath solution can be explained by an increase in surface charge density and the resulting negative shift of the voltage-dependent permeability parameters. The total absence of deactivation in Ca^{2+}-free bath requires, however, additional explanations.

2. Materials and methods

2.1. Cell culture

Mouse neuroblastoma×rat glioma hybrid cells, clone NG108-15, of passage numbers 17–36 were grown in Dulbecco's modified Eagle's medium (DMEM) supplemented with 10% fetal calf serum, 100 μM hypoxanthine, 0.4 μM aminopterin and 16 μM thymidine. For the experiments, the cells were induced to differentiate by DMEM containing 1% fetal calf serum, 100 μM hypoxanthine, 16 μM thymidine, 10 μM prostaglandin E_1 and 50 μM isobutylmethylxanthine for 5–12 days before use.

2.2. Recording of currents

Cells of 30–50 μm diameter were voltage clamped in the whole-cell mode with an EPC7 amplifier (List Electronics) using Sylgard-coated pipettes with 2–3 MΩ resistance. Series resistance was compensated ≥70%. Currents were filtered at 1–3 kHz. The volume of the recording chamber was reduced to 0.8 ml by inserting a perspex ring (internal and external diameter 15 and 35 mm, respectively) into the culture dish. The experiments were done at 20–22°C and occasionally at 33–35°C. A temperature controller from Cell MicroControls (Virginia Beach, VA) served to control the temperature.

ERG inward currents were recorded with a pulse program similar to that of [10] (see Fig. 1A). Two 0.5-s prepulses from the holding potential (−20 mV) to +20 and 0 mV, respectively, preceded the 250-ms test pulses. Test pulse potential was increased from −120 (or −140) mV in steps of 10 to 0 mV. The low holding potential and the two prepulses served to achieve maximum activation of the ERG channels. The currents elicited by the test pulses were recorded. Most of the capacitative current was compensated with an analogue circuit; leakage current was not compensated.

2.3. Solutions

Cells were continuously superfused with bath solution at a flow rate of 0.6 ml min^{-1}. ERG inward currents were recorded in bath with 40 or 6.5 mM K^+. The bath solutions contained (in mM): KCl 40, $CaCl_2$ 5, NaCl 91 or KCl 6.5, $CaCl_2$ 5, NaCl 125. When the $CaCl_2$ concentration was reduced, the NaCl concentration was increased, assuming 7.5 mM NaCl osmotically equivalent to 5 mM $CaCl_2$. Solutions with 0 $CaCl_2$ contained 0.1 or 1.1 mM EGTA. All solutions contained 10 mM Hepes (pH 7.4, adjusted with NaOH) and 0.2 μM tetrodotoxin. The composition of the pipette solution was (in mM): K-aspartate 140, KCl 30, EGTA 3, $CaCl_2$ 0.8, $MgCl_2$ 4, Na_2ATP 2, Na_2GTP 0.38, Hepes 10 (pH 7.2, adjusted with KOH); estimated free $[Ca^{2+}]$ 70–80 nM.

2.4. Analysis

For kinetic analysis, the falling phase of the ERG inward currents was fitted with one exponential according to the equation

$$I = I_{ss} + b*\exp(-t/\tau) \quad (1)$$

with the IGOR program. IGOR uses the Levenberg–Marquardt algorithm to search for the coefficient values that minimize χ^2. This is a form of non-linear, least-squares fitting.

Wherever possible, averages ± S.E.M. are given.

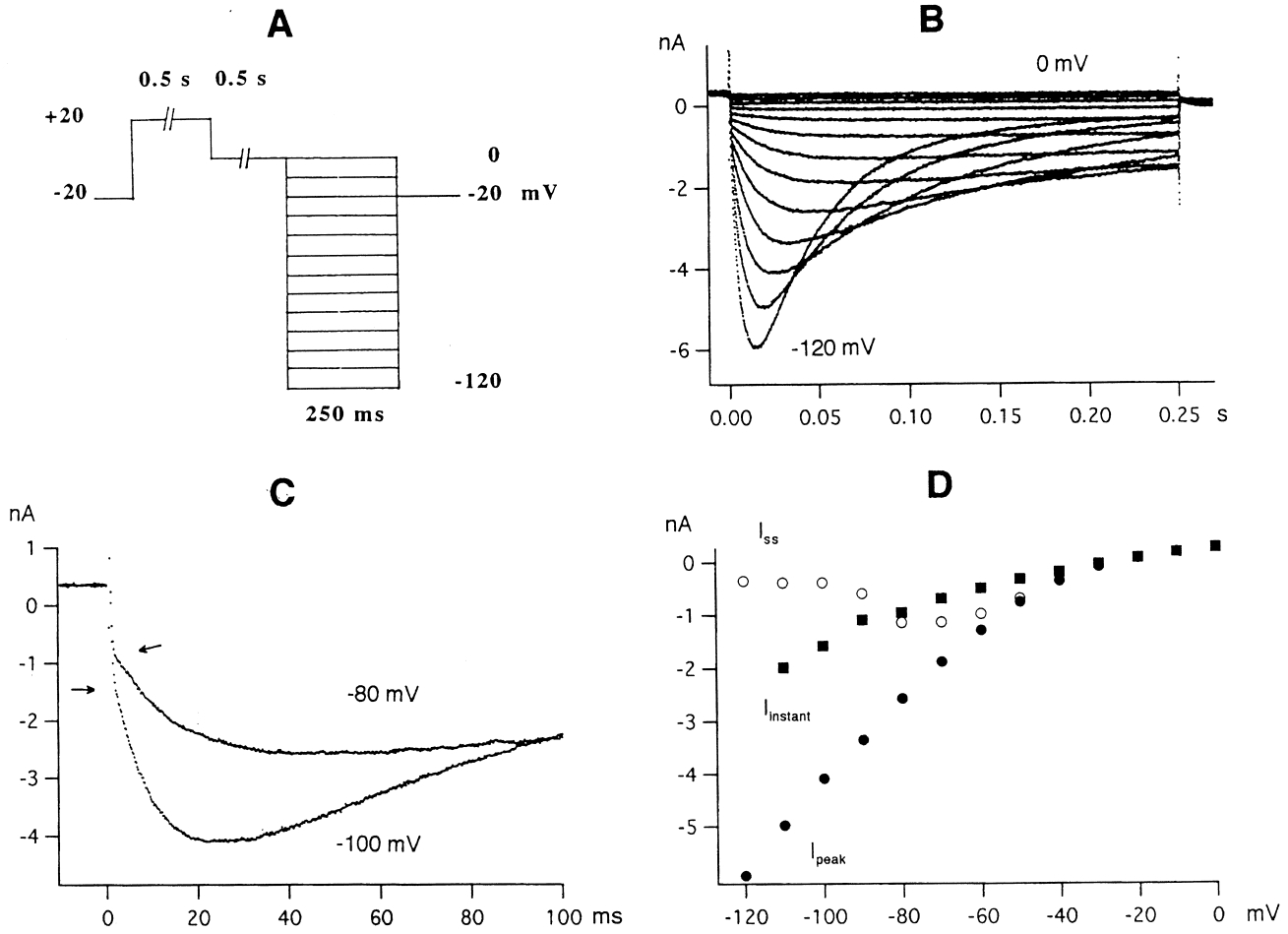

Fig. 1. ERG current in bath with 40 mM K^+ and 5 mM Ca^{2+} at 21.7°C. (A) Pulse program (see Section 2). (B) Currents recorded at pulse potentials −120 to 0 mV in steps of 10 mV. (C) Currents at −100 and −80 mV on faster time base to show the instantaneous current jump $I_{instant}$ (arrows). (D) Peak current I_{peak}, steady-state current I_{ss} and instantaneous current jump $I_{instant}$ plotted against pulse potential. I_{ss} was obtained by computer fit (Eq. 1) for pulse potentials −120 to −50 mV; for more positive pulse potentials I_{ss} was taken as the current at the pulse end. Cell diameter 41 μm.

3. Results

Fig. 1 shows ERG currents elicited by hyperpolarizing pulses in bath with 40 mM K^+, 5 mM Ca^{2+} and 0 mM Mg^{2+}. They resemble the ERG currents of neuroblastoma cells described by previous authors [4]. The currents consist of an instantaneous current jump (best seen in Fig. 1C) followed by a further increase in inward current. The inward current reaches a peak and then declines exponentially to a steady-state level. The current-voltage curves for I_{peak}, $I_{instant}$ and I_{ss} in Fig. 1D are similar to Fig. 1B of Ho et al. [5]. I_{ss} has a maximum at −70 mV and becomes smaller than $I_{instant}$ at more negative potentials.

In Fig. 1B, the rate constant of current decay (henceforth called rate constant of deactivation) is $\tau^{-1} = 24.1\ s^{-1}$ (corresponding to $\tau = 41.5$ ms) at −120 mV. Values of τ^{-1} between 20 and 25 s^{-1} at −120 mV and room temperature were obtained if care was taken to avoid series resistance artifacts. To achieve this I used preferably small cells, low resistance pipettes (< 3 MΩ) and $> 70\%$ series resistance compensation. Cells with $\tau^{-1} < 20\ s^{-1}$ were not included in the final analysis.

Fig. 2 illustrates two experiments with Ca^{2+}- (and Mg^{2+})-free bath containing 0.1 mM EGTA. In the absence of Ca^{2+}, deactivation disappeared almost completely, regardless whether the bath contained 40 mM K^+ (Fig. 2A) or 6.5 mM K^+ (Fig. 2B). Dis-

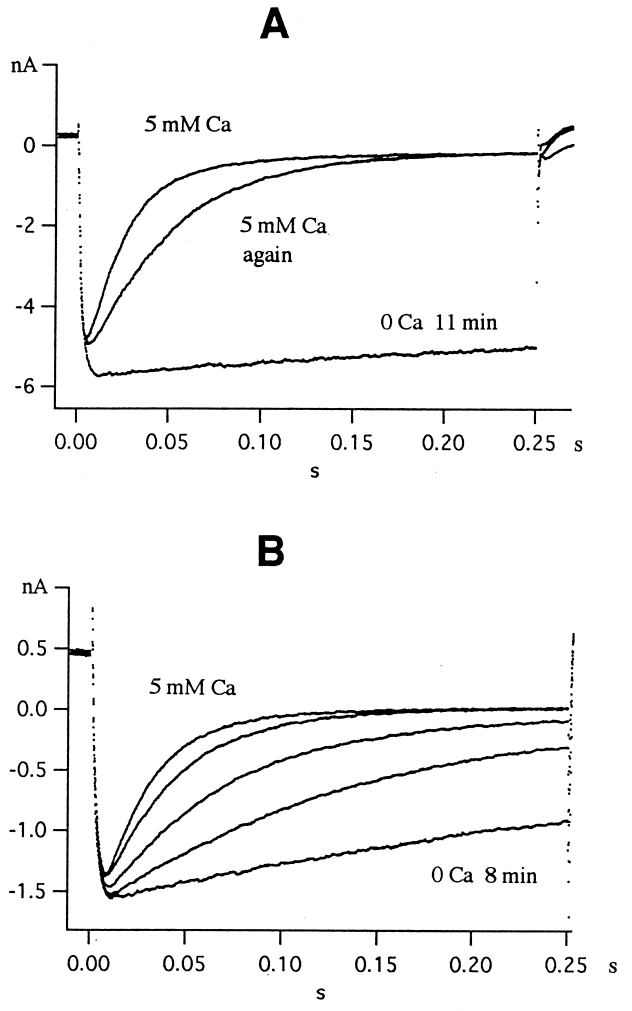

Fig. 2. Disappearance of deactivation in Ca^{2+}-free bath. (A) Cell in 40 mM K^+ bath with 5 mM Ca^{2+} and 0 Ca^{2+} at 34.4°C; records taken in 5 mM Ca^{2+}, after 11 min in 0 Ca^{2+} and 2.5 min after return to 5 mM Ca^{2+}. (B) Cell in 6.5 mM K^+ bath with 5 mM Ca^{2+} and 0 Ca^{2+} at 34.5°C; records taken in 5 mM Ca^{2+} and after 2, 3, 4 and 8 min in 0 Ca^{2+}. Pulse potential always −120 mV. Cell diameter 45 μm in A and B.

appearance of deactivation was accompanied by an increase of the peak current. The phenomenon was observed on a total of 23 cells in bath with 40 or 6.5 mM K^+ at 19.8–21.7°C or 32.8–34.8°C. Raising the temperature favored the disappearance of deactivation in Ca^{2+}-free bath. In five experiments, deactivation did not disappear in Ca^{2+}-free bath at 21°C, but almost horizontal currents were readily obtained at 34°C. They remained almost horizontal when the temperature was returned to 21°C. This observation suggests that removal of Ca^{2+} from the vicinity of the channel is facilitated by higher temperature (see Section 4).

The currents in Ca^{2+}-free bath were not exactly horizontal but decayed very slowly. Average values for the slope of this residual decay are collected in Table 1. The slope was practically the same whether the bath contained 40 or 6.5 mM K^+. Also, it did not vary with temperature between 20°C and 34°C. At 19.8–21.7°C and a pulse potential of −120 mV the average slope in 40 mM K^+, 0 Ca^{2+} was 2.70 nA/s. In bath with 5 mM Ca^{2+}, currents with a similar slope were recorded at pulse potentials of −80 or −70 mV; i.e., a voltage shift of −40 or −50 mV would have to be assumed to explain the almost horizontal currents in Ca^{2+}-free bath (see Section 4).

Upon return to 5 mM Ca^{2+}, I_{peak} was often larger than before application of Ca^{2+}-free bath, presumably because $I_{instant}$ was larger. In the experiment of Fig. 2A and in the two experiments included in Table 2, the change in I_{peak} was fully reversible.

Lowering $[Ca^{2+}]_o$ from 5 to 1.5 or 0.5 mM for 4 min was sufficient to produce clear changes in the size and time course of the ERG current. Fig. 3A,B shows currents from the same cell in 5 and 1.5 mM Ca^{2+}. Bath with 1.5 mM Ca^{2+} increased peak current and time to peak and decreased the rate constant of deactivation τ^{-1} (Fig. 3C–E). I_{peak} increased by 26% at −80 mV and by 25% at −120 mV (Fig. 3C). In 1.5 mM Ca^{2+}, the curves relating time to peak and τ^{-1} to potential were shifted by −12 and −15 mV, respectively (Fig. 3D,E). $I_{instant}$ increased only slightly (from −0.33 to −0.36 nA at −70 mV). Bath with 1.5 mM Ca^{2+} also augmented the steady-state current and shifted its maximum (see below). The effect of 1.5 mM Ca^{2+} was to a large extent reversible: 4 min after returning to 5 mM Ca^{2+} τ^{-1} at −120 mV had re-increased to 24.0 s^{-1};

Table 1
Effect of $[K^+]_o$ and temperature on the slope of the residual current decay in divalent cation-free bath with 0.1 or 1.1 mM EGTA applied for 3–14 min

Bath	Temperature (°C)	n	Slope (nA s^{-1})
40 mM K^+	32.8–34.8	7	2.42 ± 0.44
40 mM K^+	19.8–21.7	11	2.70 ± 0.36
6.5 mM K^+	33.8–34.5	3	3.15 ± 0.75
6.5 mM K^+	20.7–21.1	2	2.50 ± 0.00

Pulse potential −120 mV.

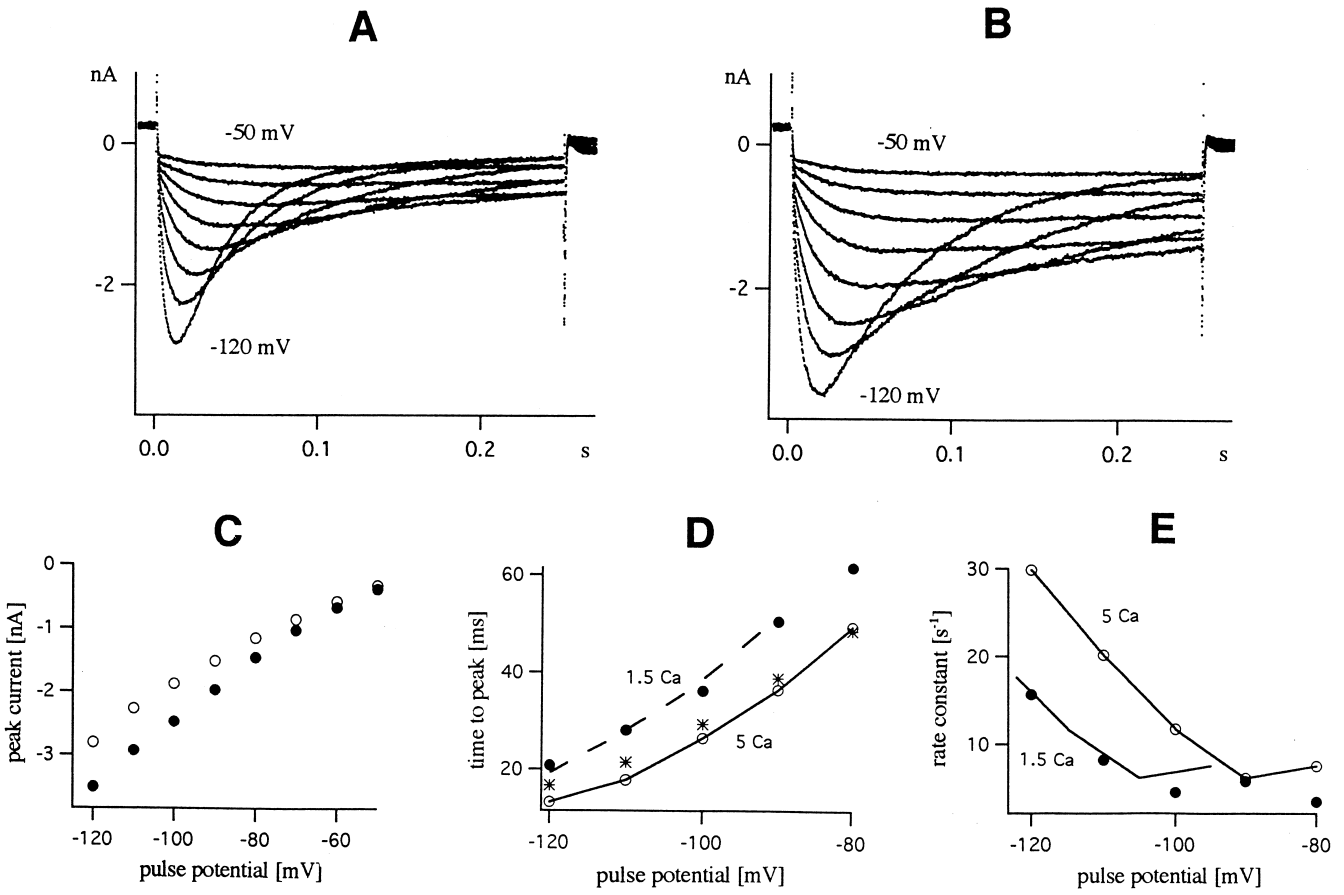

Fig. 3. ERG current in 40 mM K^+ bath with 5 and 1.5 mM Ca^{2+} at 21.3°C. (A,B) Currents recorded at pulse potentials −120 to −50 mV in steps of 10 mV in bath with 5 mM Ca^{2+} (A) or 1.5 mM Ca^{2+} (B). (C–E) Peak current, time to peak and rate constant of deactivation plotted against pulse potential for 5 mM Ca^{2+} (○) and 1.5 mM Ca^{2+} (●). For time to peak, values measured after return to 5 mM Ca^{2+} are also given (*). In D and E curves are drawn through points ○ and shifted by −12 mV (in D) or −15 mV (in E) to fit points ●. Cell diameter 38 μm.

likewise, the time to peak had decreased again (asterisk in Fig. 3D).

In the experiment of Fig. 4, the potential range was extended to −140 mV. $[Ca^{2+}]_o$ was lowered from 5 to 1.5 to 0.5 mM and then returned to 5 mM (asterisk; one value only). As seen in Fig. 4A, τ^{-1} decreased in 1.5 mM Ca^{2+} and further decreased in 0.5 mM Ca^{2+}; upon return to 5 mM Ca^{2+} τ^{-1} at −140 mV returned to a value close to the original value. Shifting the curve through 0 by −14 and −22 mV, respectively, produces curves which fit points ● and ■. Repeating the experiment of Fig. 4A on several other cells, average shifts of −14.6 ± 1.5

Table 2
Effect of lowering $[Ca^{2+}]_o$ on the deactivation rate constant τ^{-1}, the peak current I_{peak} and the difference ($I_{peak} - I_{instant}$)

Ca^{2+} (mM)	n	$\Delta\tau^{-1}$ (%)	ΔI_{peak} (%)	$\Delta(I_{peak} - I_{instant})$(%)
1.5	11	−44.3 ± 4.7[a]	+26.8 ± 3.7[c]	+47.7 ± 10.8 (n = 7)
0.5	8	−66.8 ± 5.6[b]	+28.5 ± 3.7[d]	+51.7 ± 7.2 (n = 6)
0	2		+45.0 ± 0	+49.0 ± 19.0 (n = 2)

Pulse potential −120 mV. $[K^+]_o$ = 40 mM. Temperature 21–22°C. Values give the percentage change of τ^{-1}, I_{peak} and ($I_{peak} - I_{instant}$) relative to control values measured in 5 mM Ca^{2+}. The average τ^{-1} in control was 22.6 ± 0.7 s^{-1} (n = 17). Difference between superscripts a and b significant at the 0.05 level (t-test), difference between c and d not significant.

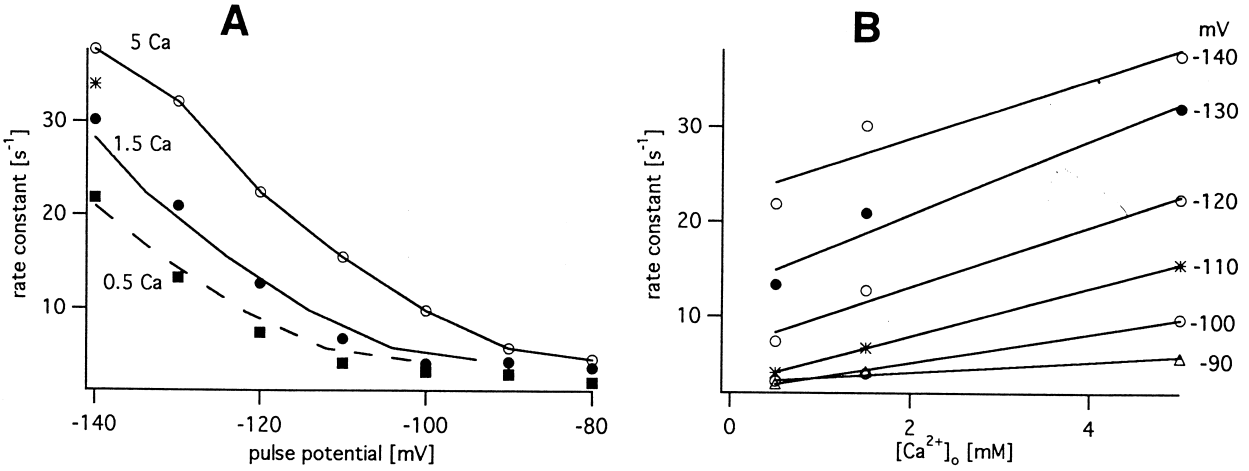

Fig. 4. Deactivation rate constant τ^{-1} as function of potential and $[Ca^{2+}]_o$ in bath with 40 mM K^+ at 21.7°C. (A) τ^{-1} versus potential for 5 mM (○), 1.5 mM (●), 0.5 mM (■) and again 5 mM (*) Ca^{2+}. Curve through ○ is shifted by −14 and −22 mV, respectively, to fit points ● and ■. (B) Same τ^{-1} values plotted versus $[Ca^{2+}]_o$ for six different potentials. Lines have slopes of 3.16, 3.92, 3.18, 2.51, 1.49 and 0.56 $mM^{-1}\,s^{-1}$ from top to bottom. Cell diameter 45 μm.

mV ($n=9$) in 1.5 mM Ca^{2+} and -20.0 ± 3.0 mV ($n=7$) in 0.5 mM Ca^{2+} were obtained.

The effect of $[Ca^{2+}]_o$ on τ^{-1} in Fig. 4A is small at −100 to −80 mV and larger at more negative potentials. To test for voltage-dependence I followed the procedure of Ho et al. [5]. I plotted τ^{-1} against $[Ca^{2+}]_o$ for six different potentials and fitted the data by lines (Fig. 4B). The slope of the lines (see numerical values in the legend of Fig. 4) was independent of voltage at −140 to −120 mV and decreased at more positive potentials. Three similar experiments confirmed this finding. This type of voltage dependence is expected if lowering $[Ca^{2+}]_o$ shifts the τ^{-1}(V) curve to the left.

As mentioned above, lowering $[Ca^{2+}]_o$ also augmented the steady-state current I_{ss} and shifted its maximum. Fig. 5 shows the U-shaped current–voltage curves of I_{ss}, sometimes called 'window current' [11]. In Fig. 5A, which is from the same experiment as Fig. 3, lowering $[Ca^{2+}]_o$ from 5 to 1.5 mM shifted

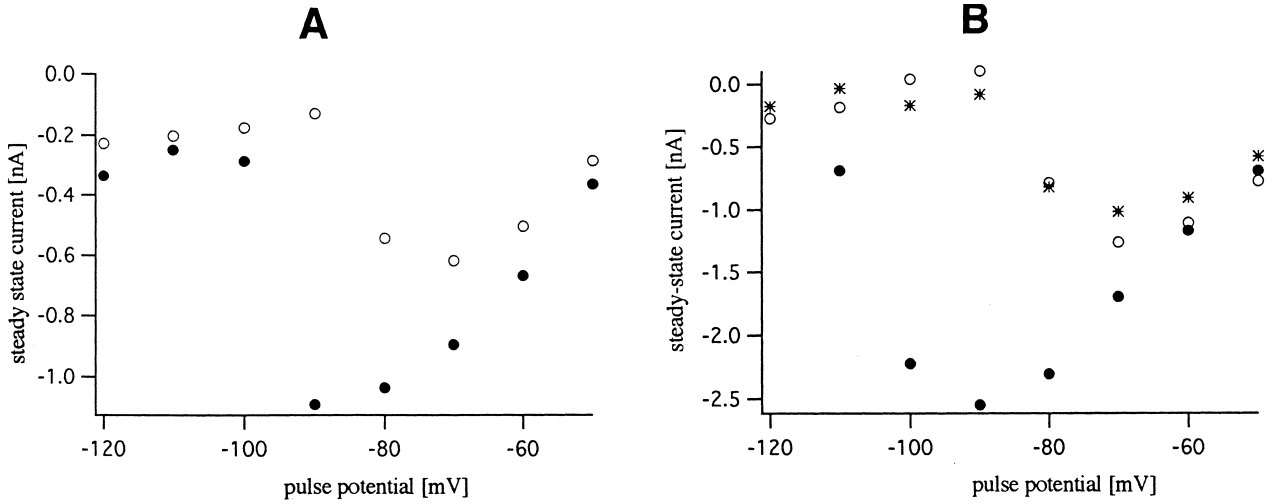

Fig. 5. Steady-state current I_{ss} in 40 mM K^+ bath with 5, 1.5 and 0.5 mM Ca^{2+}. (A) Bath with 5 mM (○) and 1.5 mM (●) Ca^{2+} at 21.3°C. Same experiment as Fig. 3. (B) Bath with 5 mM (○), 0.5 mM (●) and again 5 mM (*) Ca^{2+} at 34.3°C. Cell diameter 49 μm. I_{ss} was obtained by computer fit (Eq. 1).

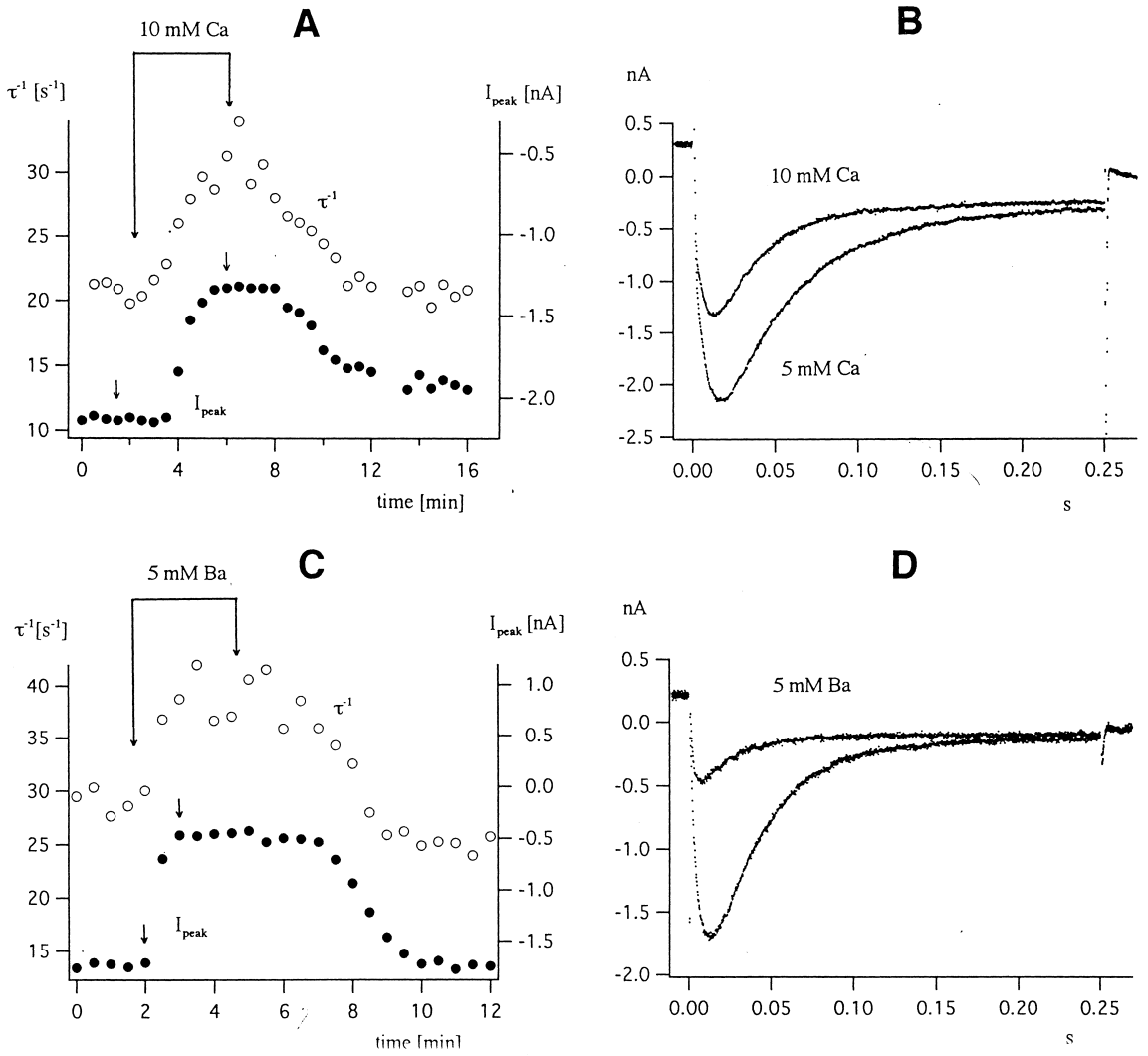

Fig. 6. Effect of increasing $[Ca^{2+}]_o$ or adding Ba^{2+} on ERG current in 40 mM K^+ bath. The same pulse (pulse potential −120 mV) was given every 30 s. (A) Deactivation rate constant (left ordinate scale) and peak current (right ordinate scale) versus time. Bath with 10 mM Ca^{2+} applied as indicated. (B) Original currents in 5 and 10 mM Ca^{2+} (see arrows in A). Cell diameter 41 μm. (C,D) A similar experiment on another cell (diameter also 41 μm) with 5 mM Ba^{2+} added to the bath.

the voltage dependence of I_{ss} by −20 mV and increased the maximum I_{ss} from −0.62 to −1.09 nA (factor 1.77). The experiment of Fig. 5B was done at a higher temperature (34.3°C), allowing a more accurate determination of I_{ss}. In this case, $[Ca^{2+}]_o$ was lowered from 5 to 0.5 mM. The maximum of I_{ss} was again shifted by −20 mV and increased from −1.25 to −2.55 nA (factor 2.04).

As expected, increasing $[Ca^{2+}]_o$ from 5 to 10 mM had an effect opposite to that of lowering $[Ca^{2+}]_o$: I_{peak} became smaller and τ^{-1} larger (Fig. 6A). The currents in Fig. 6B show a slight shortening of the time to peak (from 17.8 ms in 5 mM Ca^{2+} to 13.6 ms in 10 mM Ca^{2+}). Adding 5 mM Ba^{2+} to the bath had an effect similar to that of increasing Ca^{2+} (Fig. 6C,D), but the reduction of I_{peak} was stronger (cf. [12]).

The experiments of Figs. 3–6 are representative for a number of similar experiments. Table 2 summarizes the effects of lowering $[Ca^{2+}]_o$ on τ^{-1}, measured at −120 mV and expressed in percent of the value in 5 mM Ca^{2+}. It also contains average values for the

Table 3
Effect of increasing $[Ca^{2+}]_o$ or adding Mg^{2+} or Ba^{2+} to the bath

Bath	n	$\Delta\tau^{-1}$ (%)	ΔI_{peak} (%)
$[Ca^{2+}]$ increased to 10 mM	6	$+32.8 \pm 6.2^a$	-23.0 ± 3.6^c
5 mM Mg^{2+} added	4	$+4.3 \pm 4.3^b$	14.0 ± 1.4^d
5 mM Ba^{2+} added	5	$+32.4 \pm 5.9$	-66.2 ± 6.4^e

Pulse potential −120 mV. $[K^+]_o = 40$ mM. Temperature 21–22°C. Values give the percentage change of τ^{-1} and I_{peak} relative to control values measured in 5 mM Ca^{2+}. Differences between superscripts a and b and between c and e significant at the 0.05 level (*t*-test), difference between c and d not significant.

increase of I_{peak} in bath with 1.5, 0.5 or 0 mM Ca^{2+}. Solutions were usually applied for 5 min. When the instantaneous current jump $I_{instant}$ could be accurately measured, the difference ($I_{peak} - I_{instant}$) was calculated. It changed in the same sense as I_{peak}, but the changes were more pronounced. Effects produced by adding 5 mM Ca^{2+}, Mg^{2+} or Ba^{2+} to the bath are collected in Table 3. Ba^{2+} accelerated deactivation like Ca^{2+} but reduced I_{peak} significantly stronger, while Mg^{2+} had a relatively weak effect on both parameters.

4. Discussion

The main observations are as follows. (1) Lowering $[Ca^{2+}]_o$ from 5 to 1.5 or 0.5 mM decreases τ^{-1}, the rate constant of deactivation. The effect can be explained by a shift of the $\tau^{-1}(V)$ curve to more negative potentials. The time to peak curve and the maximum of the steady-state inward current are also shifted in the same direction. (2) Deactivation of ERG current becomes very slow in Ca^{2+}-free bath with EGTA regardless of whether $[K^+]_o$ is 40 or 6.5 mM. (3) Deactivation is clearly accelerated by increasing $[Ca^{2+}]_o$ or adding Ba^{2+} to the bath, while Mg^{2+} is less effective.

The shifts observed upon lowering $[Ca^{2+}]_o$ from 5 to 1.5 or 0.5 mM are consistent with an increase in surface charge density (see Section 1). The average shifts of the τ^{-1}(V) curve (−14.6 mV in 1.5 mM Ca^{2+}, −20.0 mV in 0.5 mM Ca^{2+}) are similar to the Ca^{2+}-dependent shifts of the sodium permeability curves of nerve fibers in Fig. 1 of [13] and Fig. 3 of [14]. According to [13,14], Mg^{2+} and Ba^{2+} have less effect on surface charge than Ca^{2+}. In my experiments on ERG currents, Mg^{2+} is also less effective than Ca^{2+} whereas adding 5 mM Ba^{2+} or 5 mM Ca^{2+} to the bath accelerates deactivation to the same extent.

According to Fig. 1 of [13] and Fig. 3 of [14], lowering $[Ca^{2+}]_o$ from 0.5 to 0 mM produces little further shift. Therefore, the shift of the $\tau^{-1}(V)$ curve in 0 Ca^{2+} (with EGTA) will not be much greater than the −20 mV observed in 0.5 mM Ca^{2+}. However, as mentioned above, a shift of −40 or −50 mV would be required to explain the almost horizontal currents in Ca^{2+}-free bath. Thus, a different explanation, in addition to the change in surface charge, must be sought. As suggested for the squid axon K^+ channel [9], Ca^{2+} and K^+ (or another monovalent cation) compete for a site R at the channel which must be occupied by Ca^{2+} if deactivation is to occur. The exchange reaction

$$CaR + 2K^+ \rightarrow K_2R + Ca^{2+}$$

would be favored by raising the temperature, explaining why deactivation is more easily abolished at higher temperature.

As shown in Tables 2 and 3, the peak current increases when $[Ca^{2+}]_o$ is lowered and decreases when Ca^{2+}, Mg^{2+} or Ba^{2+} is added to the bath. The inhibition was particularly strong in the case of Ba^{2+}, confirming previous observations on neuroblastoma cells [12]. In general, divalent and trivalent cations inhibit current flow through ion channels. For instance, lowering $[Ca^{2+}]_o$ increases the sodium permeability of nerve fibers (in addition to shifting its voltage dependence) and raising $[Ca^{2+}]_o$ decreases it [14,15]. Changes in I_{peak} could simply result from the kinetic changes caused by the divalent cations [6]. When deactivation is slowed, I_{peak} and time to peak will increase. In this case, the change in peak current should parallel the change in τ^{-1}. This was, however, not observed: 5 mM Ba^{2+} produced the same increase in τ^{-1} as adding 5 mM Ca^{2+} to the bath but caused a much stronger decrease of I_{peak} (Table 3).

My results on ERG currents of NG108-15 cells can be compared with observations on the delayed rectifier current I_{Kr} of rabbit sino-atrial node cells

which is encoded by ERG [5] and on ERG channels expressed in Chinese hamster ovary (CHO) cells [6] or *Xenopus* oocytes [16]. The comparison reveals agreement in some respects and disagreement in others. (1) My absolute τ^{-1} values are comparable to those of [6] but much smaller than those of [5]. At −100 mV and room temperature, τ^{-1} is 10–12 s^{-1} in 5 mM Ca^{2+} in my Figs. 3E and 4A and 20–27 s^{-1} in 1.8–10 mM Ca^{2+} in Fig. 3D of [6]. By contrast, τ^{-1} at −100 mV and 35°C is 120 s^{-1} in 5 mM Ca^{2+} in Fig. 3b of [5]. The difference can hardly be explained by the higher temperature alone. (2) The Ca^{2+} sensitivity of τ^{-1} reported by [6] is much smaller than in my experiments and those of [5]. Lowering $[Ca^{2+}]_o$ from 5 to 0.5 mM reduces τ^{-1} (at −120 mV) by 66.8% in Table 2 and τ^{-1} (at −100 mV) by 72.5% in Fig. 3b of [5]. However, changing $[Ca^{2+}]_o$ from 10 to 1.8 mM in Fig. 3D of [6] decreases τ^{-1} (at −100 mV) only from 27 to 20 s^{-1}, i.e., by 26%. In keeping with their lower Ca^{2+} sensitivity, ERG channels expressed in CHO cells continue to deactivate in Ca^{2+}-free bath [6]. (3) Mg^{2+} has a weaker effect than Ca^{2+} on the rate of current relaxation in my experiments as in [5]. The observation that Ba^{2+} accelerates current decay and inhibits peak current [16] agrees with my findings.

5. Conclusion

My experiments are compatible with the view that deactivation is a voltage-dependent gating process and its voltage dependence varies with $[Ca^{2+}]_o$ according to the change in surface charge density. To explain the almost horizontal currents in a Ca^{2+}-free bath with EGTA, an additional role of Ca^{2+} as cofactor for channel closing is postulated. The view that deactivation results from voltage-dependent blocking by Ca^{2+} (and Mg^{2+}) [5] is not supported by my experiments. The relation between τ^{-1} and $[Ca^{2+}]_o$ has a slope which is voltage-independent between −140 and −120 mV (Fig. 4B). A recent study on HERG channels expressed in *Xenopus* oocytes [17] comes to a similar conclusion with regard to cobalt ions: the fast deactivation produced by Co^{2+} reflects a shift in the voltage dependence of τ^{-1} rather than voltage-dependent blockade, as claimed by [16].

Acknowledgements

I am grateful to Dr M. Nirenberg (Bethesda, MD, USA) and the European Collection of Cell Cultures (Salisbury, Wiltshire, UK) for providing the NG108-15 cells. This work was supported by the Deutsche Forschungsgemeinschaft (Me 131/22).

References

[1] T. Shibasaki, Conductance and kinetics of delayed rectifier in nodal cells of the rabbit heart, J. Physiol. 387 (1987) 227–250.
[2] P.L. Smith, T. Baukrowitz, G. Yellen, The inward rectification mechanism of the HERG cardiac potassium channel, Nature 379 (1996) 833–836.
[3] P.S. Spector, M.E. Curran, A. Zou, M.T. Keating, M.C. Sanguinetti, Fast inactivation causes rectification of the I_{Kr} channel, J. Gen. Physiol. 107 (1996) 611–619.
[4] L. Faravelli, A. Arcangeli, M. Olivotto, E. Wanke, A HERG-like K^+ channel in rat F-11 DRG cell line: pharmacological identification and biophysical characterization, J. Physiol. 496 (1996) 13–23.
[5] W.-K. Ho, Y.E. Earm, S.H. Lee, H.F. Brown, D. Noble, Voltage- and time-dependent block of delayed rectifier K^+ current in rabbit sino-atrial node cells by external Ca^{2+} and Mg^{2+}, J. Physiol. 494 (1996) 727–742.
[6] J.P. Johnson Jr., F.M. Mullins, P.B. Bennett, Human *ether-à-go-go*-related gene K^+ channel gating probed with extracellular Ca^{2+}. Evidence for two distinct voltage sensors, J. Gen. Physiol. 113 (1999) 565–580.
[7] B. Frankenhaeuser, A.L. Hodgkin, The action of calcium on the electrical properties of squid axons, J. Physiol. 137 (1957) 218–244.
[8] H. Meves, J.R. Schwarz, I. Wulfsen, Separation of M-like current and ERG current in NG108-15 cells, Br. J. Pharmacol. 127 (1999) 1213–1223.
[9] C.M. Armstrong, D.R. Matteson, The role of calcium ions in the closing of K channels, J. Gen. Physiol. 87 (1986) 817–832.
[10] C.K. Bauer, The erg inwardly rectifying K^+ current and its modulation by thyrotrophin-releasing hormone in giant clonal rat anterior pituitary cells, J. Physiol. 510 (1998) 63–70.
[11] H.I. Akbarali, H. Thatte, X.D. He, W.R. Giles, R.K. Goyal, Role of HERG-like K^+ currents in opossum esophageal circular smooth muscle, Am. J. Physiol. 277 (1999) C1284–C1290.
[12] A. Arcangeli, L. Bianchi, A. Becchetti, L. Faravelli, M. Coronnello, E. Mini, M. Olivotto, E. Wanke, A novel inward-rectifying K^+ current with a cell-cycle dependence governs the resting potential of mammalian neuroblastoma cells, J. Physiol. 489 (1995) 455–471.
[13] B. Hille, A.M. Woodhull, B.I. Shapiro, Negative surface

charge near sodium channels of nerve: divalent ions, monovalent ions, and pH, Philos. Trans. R. Soc. Lond. B 270 (1975) 301–318.
[14] T. Brismar, The effect of divalent and trivalent cations on the sodium permeability of myelinated nerve fibres of *Xenopus laevis*, Acta Physiol. Scand. 108 (1980) 23–29.
[15] W. Vogel, Calcium and lanthanum effects at the nodal membrane, Pflügers Arch. 350 (1974) 25–39.
[16] W.-K. Ho, I. Kim, C.O. Lee, J.B. Youm, S.H. Lee, Y.E. Earm, Blockade of HERG channels expressed in *Xenopus laevis* oocytes by external divalent cations, Biophys. J. 76 (1999) 1959–1971.
[17] J.A. Sanchez-Chapula, M.C. Sanguinetti, Altered gating of HERG potassium channels by cobalt and lanthanum, Pflügers Arch. 440 (2000) 264–274.